Published in final edited form as:
Am J Transplant. 2010 November ; 10(11): 2396–2409. doi:10.1111/j.1600-6143.2010.03272.x.

An MHC-defined primate model reveals significant rejection of bone marrow after mixed-chimerism induction despite full MHC matching

Christian P. Larsen[1], **Andrew Page**[1], **Kelly Hamby Linzie**[1], **Maria Russell**[1], **Taylor Deane**[1], **Linda Stempora**[1], **Elizabeth Strobert**[2], **Maria Cecilia T. Penedo**[3], **Thea Ward**[3], **Roger Wiseman**[4], **David O'Connor**[4], **Weston Miller**[5,#], **Sharon Sen**[1], **Karnail Singh**[1], and **Leslie S. Kean**[5,*]

[1]The Emory Transplant Center, Department of Surgery, Emory University School of Medicine, Atlanta, GA 30322

[2]The Yerkes National Primate Research Center, Emory University, Atlanta, GA 30322

[3]Veterinary Genetics Laboratory, University of California, Davis, Davis California, 95616

[4]Wisconsin National Primate Research Center, University of Wisconsin-Madison, Madison WI, 53715

[5]Aflac Cancer Center and Blood Disorders Service, Department of Pediatrics and The Emory Transplant Center, Department of Surgery, Emory University School of Medicine, Atlanta, GA 30322

Abstract

In murine models, mixed hematopoietic chimerism-induction leads to robust immune tolerance. However, translation to primates and to patients has been difficult. In this study, we used a novel MHC-defined rhesus macaque model to examine the impact of MHC matching on the stability of costimulation blockade/sirolimus-mediated chimerism, and to probe possible mechanisms of bone marrow rejection after non-myeloablative transplant. Using busulfan-based pre-transplant preparation and maintenance immunosuppression with sirolimus, as well as CD28- and CD154-blockade, all recipients demonstrated donor engraftment after transplant. However, the mixed-chimerism that resulted was compartmentalized, with recipients demonstrating significantly higher whole blood chimerism compared to T cell chimerism Thus, the vast majority of T cells present post-transplant were recipient- rather than donor-derived. Surprisingly, even in MHC-matched transplants, rejection of donor hematopoiesis predominated after immunosuppression withdrawal. Weaning of immunosuppression was associated with a surge of antigen-experienced T cells, and transplant rejection was associated with the acquisition of donor-directed T cell alloreactivity. These results suggest that a reservoir of alloreactive cells was present despite prior costimulation blockade and sirolimus, and that the post-immunosuppression lymphocytic rebound may have lead to a phenotypic shift in these recipient T cells towards an activated, antigen experienced phenotype, and ultimately, to transplant rejection.

[*]**Corresponding Author Contact Information:** Leslie S. Kean, 101 Woodruff Circle, NE, Room 5203, Emory University School of Medicine, Atlanta, GA 30322 Department Fax: 404-727-3660 Phone: 404-727-5265 MedLK@emory.edu.
[#]Current address: Pediatric Hematology-Oncology, University of Minnesota, Minneapolis, MN 55455

Introduction

While durable mixed chimerism-induction is well-established in mice, and is associated with tolerance to solid organ allografts, (1–7) the translation of this approach to both non-human primate (NHP) models and to patients has been less straightforward. Thus, in NHP, evidence that chimerism (transient or stable) is necessary and sufficient for tolerance after solid organ transplantation is lacking: studies of mixed-chimerism and kidney transplant in cynomolgous monkeys demonstrated renal allograft rejection both in the presence and absence of transient bone marrow chimerism, (8,9), and studies of mixed-chimerism and lung transplantation failed to show a chimerism-mediated prolongation of allograft acceptance. (10) In Kawai et al's recently published landmark clinical trial of combined bone marrow and kidney transplantation, prolonged kidney survival was observed in the setting of transient donor chimerism, but persistent donor chimerism was unnecessary for the creation of functional tolerance. (11) In contrast, in Scandling et al's description of the first three patients enrolled in their combined bone marrow-kidney transplant series, one patient developed stable chimerism and demonstrated tolerance to a donor kidney, while a second patient, who demonstrated transient chimerism, rejected the donated kidney. (12) Critical mechanistic questions thus remain concerning the relationship between donor chimerism and tolerance-induction, (13) including understanding the mechanisms contributing to transient versus stable chimerism, and determining whether stable chimerism, if it is achievable, will improve graft acceptance across a variety of immunosuppression platforms.

While the use of a primate model is accepted to be a critical bridge to clinical translation of mixed-chimerism-based and other therapeutic strategies for tolerance-induction, (14,15) historically, primate studies have suffered from a significant disadvantage compared to both mouse and human studies. This disadvantage is due to the fact that, until the studies reported here, primate models were characterized by their notable lack of information about either degree of relatedness or MHC disparity between primate transplant pairs. Given the impact that the degree of MHC disparity and degree of relatedness makes on both HSC engraftment and immunity to solid organ allografts, this lack of information significantly impaired our ability to draw consistent conclusions from these studies. In the studies reported here, we have made a fundamental improvement in the rigor of our rhesus macaque model of transplantation by developing two rhesus macaque colonies with defined pedigree relationships and for whom the degree of MHC haplotype matching between related animals was known.

We have used this novel resource to perform the first transplant series utilizing MHC-defined rhesus macaques to investigate the mechanisms of mixed-chimerism induction and maintenance after non-myeloablative hematopoietic stem cell transplant. In this report, we show that even after MHC-matched transplant, recipients were highly resistant to the development of significant donor T cell chimerism, and that after withdrawal of costimulation blockade and sirolimus, there was a high risk of rejection of the donor hematopoietic cells. These results suggest that a reservoir of alloreactive recipient T cells were present that were resistant to prior treatment with costimulation blockade/sirolimus and to mixed-chimerism, and that the expansion of these cells after immunosuppression withdrawal functioned to increase the risk of transplant rejection.

Materials and Methods

Experimental animals

This study used rhesus macaques from either the Yerkes National Primate Research Center or the NIH-sponsored rhesus macaque colony at Yemassee, SC, managed by Alphagenesis, Inc. Animals were treated according to IACUC and ALAC guidelines.

Establishment of an MHC-defined Rhesus macaque transplant model

The establishment of two MHC-defined Rhesus macaque colonies is described in detail in the Supplementary Material.

Transplant Preparation and Immunosuppression Strategy

The transplant strategy employed was essentially the same as described previously. (16) As shown in Figure 1a, it included a single pre-transplant dose of busulfan (9.5 mg/kg, Otsuka America Pharmaceutical, Rockville, MD), two peri-transplant doses of basiliximab (0.3mg/kg/dose) and maintenance immunosuppression with sirolimus (LC Laboratories, Woburn, MA, serum trough levels targeted at 5–15mg/mL), the anti-CD154 antibody, H106, and the CD28 blockade agent LEA29Y (H106 and LEA29Y provided by Bristol Myers Squibb, Pennington, NJ.). The dosing strategies for H106 and LEA29Y were as follows: H106: Day −6, −4, −1, 1, 3, 7, 9, 11, 14, 21, 35, 49, 63, 77, 91, 119, 147, 175. LEA29Y: Day −6, −4, −1, 3, 7, 11, 14, 21, 35, 49, 63, 77, 91, 119, 147, 175. Sirolimus was continued throughout the treatment course with costimulation blockade, with the sirolimus wean planned for a one-month period after the last dose of costimulation blockade was given. For three animals, RDe9, RCh9 and RFo9, costimulation blockade was discontinued at day +150 due to systemic illness (from which they recovered) with weaning of sirolimus shortly thereafter. Of the twelve transplants performed, two of the recipients (DJ63 and DJ66) were unevaluable, as they died (on day +110 and day +161 respectively, while still chimeric and on immunosuppression) of campylobacter enterocolitis (DJ63) and cryptosporidium (DJ66).

HSCT

HSCT utilized both terminal bone marrow donation and leukopheresis-derived hematopoietic stem cells (HSC). While the initial transplants (CW54, CW55 and RDe9) were performed using bone marrow, when leukopheresis was established in our laboratory, the standard protocol for subsequent transplants was revised to use exclusively leukopheresis-derived stem cells, as this method permitted the survival of the transplant donor. Both bone marrow and leukopheresis-based HSC collections were performed as previously described (16) and the products analyzed for: (i) total nucleated cell dose, (ii) $CD34^+$ cell dose, (iii) $CD3^+$ T-cell dose, (iv) $CD4^+$ T-cell dose, (v) $CD8^+$ T-cell dose. Analysis was performed either by automated CBC or by flow cytometric analysis with anti-CD34 (clone 563), anti-CD3 (clone SP34), anti-CD4 (clone SK3), anti-CD8 (clone SK1, all from Pharmingen San Jose, CA). The composition of the HSC grafts for all recipients is shown in Table 1.

Chimerism determination

When appropriate for specific donor:recipient mismatches, MHC- or SRY-based chimerism was monitored by real-time SybrGreen PCR (ABI, Foster City, CA) as previously described. (16) If PCR-based chimerism determination was not possible, divergent donor-and recipient-specific microsatellite markers were used, (17) by comparing peak-heights of the donor- and recipient-specific amplicons. T cell or myeloid chimerism was determined by sorting CD3+/CD20− (T cells) or CD14+/CD45+ (myeloid cells) using a FACSAria cell sorter (Becton Dickinson, San Diego, CA) prior to molecular analysis for donor-specific microsatellite amplicons or PCR products. The day of rejection was defined as the last day that donor chimerism could be detected by PCR or microsatellite analysis.

CMV monitoring

was performed as previously described (16), and is reported as CMV copies per milliliter of whole blood. While prior immunity to CMV was not tested serologically, CMV is highly prevalent in the colonies from which these animals were derived. Thus, while not

determined conclusively, the CMV viral load that occurred post-transplant likely arose from viral reactivation.

Measuring anti-donor T-cell alloreactivity using CFSE-MLR

CFSE MLR analysis was performed as previously described. (16) To quantify the amount of proliferation that occurred, CD8+ cells were gated, and the percent of cells remaining in culture that had divided at least once (resulting in a > 2-fold reduction in CFSE fluorescence compared to the undivided fraction) was determined using FloJo flow cytometry analysis software (Ashland, OR).

Longitudinal flow cytometric analysis of T cell phenotype

Multicolor flow cytometry panels were used to determine the following cell subpopulations: T cells: CD3+/CD20−; B cells: CD20+/CD3−; CD4+ T cells: CD4+/CD3+/CD8−/CD20−; CD8+ T cells: CD8+/CD3+/CD4−/CD20−; Naïve T cells (Tn): CD28+/CD95− cells in either the CD4 or CD8 T cell subsets; central memory T cells (Tcm): CD28+/CD95+ cells in either the CD4 or CD8 T cell subsets; effector/Effector memory T cells: CD28−/CD95+ cells in either the CD4 or CD8 T cell subsets; (18) Tregs: CD4+/CD3+/FoxP3+/CD25+ cells. The sources and clones used for each of these antibodies are as follows: From BD Biosciences (San Jose CA): CD3, Clone SP34-2; CD8, Clone: RPA-T8. From eBioscience (San Diego CA): CD4, Clone OKT4; CD20, Clone: 2H7; CD28, Clone: CD28.2; CD95, Clone: DX2. FoxP3, Clone: PCH101. Longitudinal flow cytometric analysis was performed using Flojo flow cytometry analysis software.

Measurement of anti-donor antibody

The presence of anti-donor antibody was determined by incubating PBMCs from the donor with serum from the recipient which was collected either pre-transplant or after rejection. The presence of anti-donor antibody in the recipient serum was detected flow cytometrically on CD3+/CD20− cells by binding of a FITC-labeled goat anti-monkey IgG (KPL Inc, Gaithersburg, Maryland, catalog # 072-11-021) to the donor cells to which anti-donor antibodies were bound.

Statistical Analysis

Anova and Kaplan-Meier analysis was carried out using the JMP® statistical software package, Version 8 (SAS Institute Inc, Cary, NC, 1989–2009). To determine Anova for multiple parameters, a post-hoc Tukey HST test was used to determine significant differences for pair-wise comparisons.

Results

MHC similarity predicts length of engraftment of donor hematopoietic cells after non-myeloablative BMT

Having established the MHC-defined rhesus macaque colonies (described in detail in Supplementary Material), we were able to use animals from these colonies to rigorously determine the impact that MHC haplotype sharing had on the durability of mixed chimerism after non-myeloablative hematopoietic stem cell transplantation. Figure 1a shows the pre-transplant preparative and immunosuppression strategy that was employed. Figure 1b,c shows the chimerism time course for all treated animals, while Figure 1d shows Kaplan-Meier analysis comparing allograft survival for the one MHC haplotype matched cohort with allograft survival in the two MHC haplotype matched cohort. This analysis confirmed that increasing MHC matching resulted in a statistically significant prolongation in engraftment ($p=0.0018$). Figure 1e shows a longitudinal analysis of CMV viral load in the

transplanted animals, confirming that immune competence, as measured by control of viral infection or reactivation, was also improved in this MHC-matched cohort compared to historical controls. (16) Several conclusions can be drawn from the longitudinal analysis of chimerism in the two transplant cohorts (Figure 1). First, post-transplant immunosuppression was necessary for the development of chimerism, as the untreated control (CW7A) failed to exhibit donor engraftment. Second, for both cohorts (one MHC haplotype-matched and two MHC haplotype-matched) receiving sirolimus/costimulation-blockade-based post-transplant immunosuppression, significant whole blood chimerism could be established. Third, while the one MHC-haplotype matched cohort uniformly lost chimerism despite ongoing immunosuppression, the two MHC-haplotype matched cohort routinely maintained chimerism for a period of time after immunosuppression withdrawal. However, with the exception of one recipient, RDe9, who has become a long-term chimera, donor engraftment was eventually lost with the time of immunosuppression-free chimerism ranging from 14 days (animal RCq7) to 168 days (animal DK8B).

Rejection was accompanied by the appearance of robust donor-directed alloreactivity

As shown in the representative CFSE MLR analysis for RCq7 in Figure 2, at day 135, during immunosuppressive treatment, and in the presence of donor chimerism, minimal donor-specific alloproliferation was observed (0.49%), while alloproliferation to a third-party stimulus was preserved. However, at day +266, after rejection, CFSE MLR analysis revealed the acquisition of robust alloproliferation (12.4%). Importantly, in RDe9, the one recipient who has maintained donor chimerism for >1665 days, donor specific alloproliferation remained blunted after immunosuppression withdrawal (Figure 2) while alloproliferation to third-party antigens persisted, consistent with donor-specific tolerance in the setting of immune competence to other antigens.

Compartmentalized chimerism occurred after transplant

The observation of anti-donor T cell alloreactivity predicted that a significant proportion of recipient T cells persisted after transplant. To test this, we sorted T cells flow cytometrically and determined their level of chimerism using molecular techniques. As shown in Figure 3a, T cell chimerism was consistently lower than whole blood chimerism for all transplant recipients. The high levels of whole blood chimerism that were measured (Figure 1c) thus reflected non-T cell chimerism, which was predominantly myeloid-derived. Thus, as shown in the representative example in Figure 3b, sorted myeloid chimerism closely mirrored whole blood chimerism. This is expected, given the predominance of CD14+ granulocytes in whole blood post-transplant. Given this result, myeloid cells were not routinely sorted for analysis, and T cell chimerism was compared to whole blood chimerism for all transplanted animals. Consistent with the lack of high levels of T cell chimerism, and the ultimate development of rejection in the majority of transplant recipients, GvHD did not occur in this transplant cohort. Thus, GvHD-associated clinical findings (rash, diarrhea, hyperbillirubinemia) were not observed, all recipients maintained their pre-transplant weights, and none of the animals who died post-transplant had histopathologic signs of GvHD (not shown).

A surge in recipient lymphocyte counts accompanied immunosuppression withdrawal and preceded transplant rejection

To determine if any correlation occurred between the T cell phenotype after immunosuppression withdrawal and subsequent transplant rejection, we longitudinally monitored the absolute lymphocyte count (the ALC), the absolute CD4+ T cell counts, the absolute CD8+ T cell counts as well as absolute numbers of naïve (CD28+/CD95−) central memory (CD28+/CD95+) and effector memory (CD28−/CD95+) CD4+ and CD8+ T cells in our transplant recipients. Figure 4 shows representative data for the following animals:

DK8B, RCh9, RCq7, RDe9, RFo9 and RQq9. As shown in figure 4a, we observed that when compared with pre-transplant counts, the ALC, was reduced during immunosuppression. However, in the setting of immunosuppression withdrawal, the ALC significantly rebounded, to levels as high as 7 fold greater than during immunosuppression (Figure 4a, DK8B). This increase in the ALC translated into increases in absolute CD4+ and CD8+ T cells (Figure 4b). When subpopulation analysis of CD4+ and CD8+ T cells was performed (flow cytometry gating strategy shown in Figure 4c), distinct patterns emerged for these two cell types. Thus, as shown in the representative example for RCq7 in Figure 4d, CD4+ T cells exhibited a striking shift in phenotype, with acquisition of CD95 expression, consistent with an antigen-experienced CD28+/CD95+ "Tcm" phenotype. As shown in Figure 4d, the shift in the CD8+ T cell subpopulation phenotype was less striking than that observed for CD4+ T cells, but also favored a shift toward CD95-positivity, with CD28−/CD95+ CD8+ "Tem" cells predominating. Importantly, the pattern of phenotypic shifting shown for RCq7 in Figure 6 was noted for all transplant recipients, whether stable chimerism (Rde9) or rejection (DK8B, RCh9, RCq7, RFo9, RQq9) occurred. Figure 4e demonstrates the flow cytometry profile of RQq9, in which the shift in T cell phenotype that occurred after immunosuppression withdrawal was magnified by the subsequent placement of a donor skin graft in the setting of high donor chimerism (61%), and discontinued immunosuppression. This recipient subsequently rejected both the HSC and skin allografts, consistent with a lack of immune tolerance-induction despite the long-term presence of donor hematopoiesis. In contrast to the shift in effector T cell populations noted above, neither engraftment nor rejection was accompanied by significant shifts in the balance of CD4+/CD3+/FoxP3+/CD25+ Tregs compared to bulk CD4+ T cells (Figure 4f).

Rejection occurred in the absence of anti-donor antibody development

Anti-donor antibodies were measured for recipients DK8B, RCh9, RCq7, RQq9, (treated with sirolimus and costimulation blockade) and for CW7A (the untreated control). As shown in Figure 4g, despite rejection, none of the treated animals developed anti-donor antibodies, while CW7A, the animal who was not treated with sirolimus or costimulation blockade, did demonstrate anti-donor antibody formation.

Discussion

Creating the next generation primate model: Incorporating knowledge of MHC disparity into transplant planning in macaques

Primate allogeneic transplantation models have historically suffered from a serious drawback compared to both murine models and to clinical trials: This has been the lack of information concerning both animal pedigree and degree of MHC disparity that has historically characterized these studies. However, DNA microsatellite analysis has now allowed us to fully pedigree two colonies of rhesus macaques, and, within a family unit, determine the heritability of the MHC chromosomes between parents and offspring. This advance allows us to choose transplant pairs based on their degree of relatedness and their degree of MHC disparity, something that until now, has not been possible. Our results confirm what has been shown repeatedly in murine and human studies: that the degree of MHC disparity impacts transplant outcome. Thus, this work points to an important confounder that must be acknowledged for all primate transplant studies that are performed without knowledge of MHC sharing: since transplant outcome is affected by MHC disparity, transplant success or failure cannot be attributed solely to the immunosuppressive strategy if MHC matching is not also controlled for. Pedigreed and MHC-defined colonies should, therefore, become the gold-standard for NHP transplantation studies—allowing the most rigorous investigation of novel immunosuppressive regimens without the confounder of unknown degrees of familial relatedness or MHC matching between transplant pairs.

Rejection of donor hematopoietic cells: mechanistic implications of breakthrough alloreactivity after immunosuppression withdrawal

Our results show that while CD28/CD154-directed costimulation blockade and sirolimus permit engraftment of allogeneic hematopoietic stem cells after busulfan pre-transplant preparation, even for MHC-matched transplants, this immunosuppression regimen was largely inadequate to fully tolerize recipient T cells to the donor bone marrow allograft and result in long-term, stable donor chimerism. The immunophenotype of the MHC-matched recipients, both during ongoing donor engraftment and during rejection, has allowed us to develop a model of the possible mechanisms of tolerance-resistance in the setting of T-cell-poor compartmentalized mixed-chimerism (Figure 5). This model incorporates (1) the pretransplant alloreactive T cell precursor frequency present in MHC-matched and MHC-mismatched transplants, (2) the inhibitory impact that costimulation blockade and sirolimus had on the number and function of alloreactive cells, and (3) the presence of a reservoir of costimulation blockade-resistant cells, which expand and shift phenotype after immunosuppression withdrawal, increasing the risk for rejection even after MHC-matched transplant.

While this model proposes that the expansion of memory T cells may result in the accumulation of sufficient anti-donor alloreactivity to result in graft rejection, formal proof of the relative contributions of the different memory populations will require purification of these populations and testing each individually for alloreactivity. Additionally, while the pace of transplant rejection after immunosuppression withdrawal suggests that a reservoir of pre-existing anti-donor T cells functioned prominently in graft rejection, a failure of central deletion of newly emergent donor-reactive cells also could have contributed to transplant rejection. According to this model, the compartmentalized chimerism that resulted may not have been sufficient to adequately repopulate the recipient thymus, leading to a failure to delete donor-reactive thymic emigrants after transplant.

Lessons to be learned from RDe9, the sole stable chimera

While the establishment of stable mixed-chimerism in RDe9 likely arose due to the stochastic probability that in this recipient, all alloreactive clones were eliminated, it is important to examine other possible causes of this isolated success at tolerance-induction. Although the level of T cell chimerism in RDe9 was not higher than in those recipients who ultimately rejected their allograft (Figure 3a), two characteristics of this transplant were different than the majority of the other evaluable transplant pairs.

First, RDe9 received hematopoietic stem cells from a bone marrow allograft, rather than a leukopheresis-derived allograft. While the cellular characteristics of the transplanted inoculum for RDe9 were similar to those found in the other two haplotype-matched animals (Table 1), and while two of the one MHC haplotype-matched recipients also received a bone marrow allograft without becoming tolerant, it is possible that bone marrow was required for tolerance in the MHC-matched transplants. We sought to test this hypothesis by transplanting two additional animals (DJ63 and DJ66) with bone marrow-derived stem cells, but unfortunately, both animals succumbed to an outbreak of colitis while still receiving immunosuppression. Given the relative scarcity of the two MHC haplotype-matched pairs, we have thus far been unable to add more animals to our analysis. Thus, while we think it unlikely, given the length of engraftment of the animals receiving leukopheresis-derived stem cells, and given the data from human studies that show equivalent (or improved) engraftment with PBSCs, (19–21) it remains a possibility that bone marrow-derived hematopoietic products will be more tolerogenic than leukopheresis-derived transplants.

The second distinguishing characteristic of RDe9 and her donor compared to the majority of the other transplant pairs was that this pair was sex-matched (female-to-female transplantation), in contrast to four of five of the other evaluable transplant pairs, which were sex-mismatched (Table 1). Although sex-matched transplantation did not guarantee tolerance-induction (DK8B ultimately rejected his transplant), gender-associated minor histocompatibility antigens (miHC) are well-documented to play important roles in transplant outcome, (22) and may have increased the precursor frequency of alloreactive T cells in the sex-mismatched transplant pairs. Thus, even with full MHC matching between transplant pairs, a reservoir of alloreactive cells (presumably recognizing both sex-determined and other miHCs) that were resistant to prior treatment with costimulation blockade and sirolimus, and to the presence of mixed chimerism, could persist, and cause rejection of donor bone marrow in the weeks and months after immunosuppression withdrawal.

The relationship between mixed-chimerism and solid organ transplant tolerance

Kawai et al have shown that in patients, successful withdrawal of immunosuppression can be achieved after combined bone marrow/kidney transplant in the setting of transient (<2 weeks) donor chimerism. (11) The comparison of their results with this study raises two important issues concerning the relationship between chimerism and tolerance. First, it is important to note that the intention of Kawai et al's studies (9–11) and the study described here were different. Thus, Kawai et al have used multimodal recipient conditioning and induction immunosuppression, with the goal of establishing tolerance to a renal allograft in the setting of transient mixed-chimerism. (13) In contrast, the study described here was designed to exclusively investigate whether stable mixed-chimerism could be induced in primates, in the absence of solid organ transplantation. In mice, durable mixed chimerism can be created, and this chimerism has been observed to induce tolerance to both solid organ and skin allografts. (1,2,4,6) Thus, our goal was to induce durable chimerism in primates, so that, in future studies, the impact of this chimerism on solid organ allograft acceptance could be tested. Our results suggest that in the complex, clinically relevant macaque model, a reservoir of T cells exist (even after MHC-matched transplant) that are not adequately tolerized by CD28/CD154-directed costimulation blockade or by mixed-chimerism, and that the expansion of these cells after immunosuppression withdrawal can result in rejection of donor bone marrow. The MHC-defined experimental platform that is described here should allow a thorough analysis of the mechanisms by which these recipient T cells resist tolerance, and an investigation of adjunctive strategies by which this costimulation blockade-resistant reservoir of alloreactivity might be successfully controlled.

The second issue concerns the relationship between the rejection of donor bone marrow and the survival of a concurrently placed solid organ allograft. While not tested in the present study, it is possible that split tolerance may be achievable in rhesus macaques (and patients) with combined busulfan and costimulation blockade, and that a renal transplant would have been accepted despite rejection of donor hematopoiesis. Alternatively, it is possible that the robust rejection response we observed toward donor bone marrow might trigger linked rejection of a donor kidney. This outcome would suggest that prolonged exposure of recipient T cells to donor antigens (in the form of donor myeloid chimerism) may afford more risk than benefit to the survival of solid organ allografts. These opposing hypotheses represent an important area for future investigation which can now be performed using the MHC-defined rhesus macaque transplant model.

Supplementary Material

Refer to Web version on PubMed Central for supplementary material.

Acknowledgments

The authors thank Kristy Kraemer, PhD for her administrative and scientific leadership of the MHC typing initiative for the Nonhuman Primate Transplantation Tolerance Cooperative Steering Group and Isabelle Lussier, for her significant contributions to the MHC typing initiative. The authors thank Daniel Promislow, PhD, for performing the statistical analysis for this study. LSK and CPL are members of the Children's Healthcare of Atlanta Transplant Immunology and Immune Therapeutics Center. LSK and CPL are members of the Nonhuman Primate Transplantation Tolerance Cooperative Steering Group.

Funding Sources: This work was supported by Yerkes National Primate Research Center Base Grant, #RR00165. CPL was supported by NIH grant #s 2U19 AI051731, and 2P01 AI044644. LSK was supported by grant #s 5K08 AI065822, 2U19 AI051731, and 2U24 RR018109, and by a Burroughs Wellcome Fund Career Award in the Biomedical Sciences. MCTP and TW were supported by NIH grant # U24 RR18144-01.

References

1. Adams AB, Durham MM, Kean L, Shirasugi N, Ha J, Williams MA, et al. Costimulation blockade, busulfan, and bone marrow promote titratable macrochimerism, induce transplantation tolerance, and correct genetic hemoglobinopathies with minimal myelosuppression. J Immunol. Jul 15; 2001 167(2):1103–11. [PubMed: 11441122]
2. Durham MM, Bingaman AW, Adams AB, Ha J, Waitze SY, Pearson TC, et al. Cutting edge: administration of anti-CD40 ligand and donor bone marrow leads to hemopoietic chimerism and donor-specific tolerance without cytoreductive conditioning. J Immunol. Jul 1; 2000 165(1):1–4. [PubMed: 10861026]
3. Kean LS, Durham MM, Adams AB, Hsu LL, Perry JR, Dillehay D, et al. A cure for murine sickle cell disease through stable mixed chimerism and tolerance induction after nonmyeloablative conditioning and major histocompatibility complex-mismatched bone marrow transplantation. Blood. Mar 1; 2002 99(5):1840–9. [PubMed: 11861303]
4. Larsen CP, Elwood ET, Alexander DZ, Ritchie SC, Hendrix R, Tucker-Burden C, et al. Long-term acceptance of skin and cardiac allografts after blocking CD40 and CD28 pathways. Nature. May 30; 1996 381(6581):434–8. [PubMed: 8632801]
5. Sharabi Y, Abraham VS, Sykes M, Sachs DH. Mixed allogeneic chimeras prepared by a non-myeloablative regimen: requirement for chimerism to maintain tolerance. Bone Marrow Transplant. Mar; 1992 9(3):191–7. [PubMed: 1387333]
6. Sykes M, Szot GL, Swenson KA, Pearson DA. Induction of high levels of allogeneic hematopoietic reconstitution and donor-specific tolerance without myelosuppressive conditioning. Nat Med. Jul; 1997 3(7):783–7. [PubMed: 9212108]
7. Tomita Y, Sachs DH, Sykes M. Myelosuppressive conditioning is required to achieve engraftment of pluripotent stem cells contained in moderate doses of syngeneic bone marrow. Blood. Feb 15; 1994 83(4):939–48. [PubMed: 7906567]
8. Kawai T, Cosimi AB, Colvin RB, Powelson J, Eason J, Kozlowski T, et al. Mixed allogeneic chimerism and renal allograft tolerance in cynomolgus monkeys. Transplantation. Jan 27; 1995 59(2):256–62. [PubMed: 7839449]
9. Kawai T, Sogawa H, Boskovic S, Abrahamian G, Smith RN, Wee SL, et al. CD154 blockade for induction of mixed chimerism and prolonged renal allograft survival in nonhuman primates. Am J Transplant. Sep; 2004 4(9):1391–8. [PubMed: 15307826]
10. Aoyama A, Ng CY, Millington TM, Boskovic S, Murakami T, Wain JC, et al. Comparison of lung and kidney allografts in induction of tolerance by a mixed-chimerism approach in cynomolgus monkeys. Transplant Proc. Jan–Feb; 2009 41(1):429–30. [PubMed: 19249572]
11. Kawai T, Cosimi AB, Spitzer TR, Tolkoff-Rubin N, Suthanthiran M, Saidman SL, et al. HLA-mismatched renal transplantation without maintenance immunosuppression. N Engl J Med. Jan 24; 2008 358(4):353–61. [PubMed: 18216355]
12. Scandling JD, Busque S, Dejbakhsh-Jones S, Benike C, Millan MT, Shizuru JA, et al. Tolerance and chimerism after renal and hematopoietic-cell transplantation. N Engl J Med. Jan 24; 2008 358(4):362–8. [PubMed: 18216356]

13. Kirk AD. Clinical tolerance 2008. Transplantation. Apr 15; 2009 87(7):953–5. [PubMed: 19352112]
14. Kean LS, Gangappa S, Pearson TC, Larsen CP. Transplant tolerance in non-human primates: progress, current challenges and unmet needs. Am J Transplant. May; 2006 6(5 Pt 1):884–93. [PubMed: 16611324]
15. Kirk AD. Crossing the bridge: large animal models in translational transplantation research. Immunol Rev. Dec.2003 196:176–96. [PubMed: 14617205]
16. Kean LS, Adams AB, Strobert E, Hendrix R, Gangappa S, Jones TR, et al. Induction of chimerism in rhesus macaques through stem cell transplant and costimulation blockade-based immunosuppression. Am J Transplant. Feb; 2007 7(2):320–35. [PubMed: 17241112]
17. Penedo MC, Bontrop RE, Heijmans CM, Otting N, Noort R, Rouweler AJ, et al. Microsatellite typing of the rhesus macaque MHC region. Immunogenetics. May; 2005 57(3–4):198–209. [PubMed: 15900491]
18. Pitcher CJ, Hagen SI, Walker JM, Lum R, Mitchell BL, Maino VC, et al. Development and homeostasis of T cell memory in rhesus macaque. J Immunol. Jan 1; 2002 168(1):29–43. [PubMed: 11751943]
19. Bensinger WI, Storb R. Allogeneic peripheral blood stem cell transplantation. Rev Clin Exp Hematol. Jun; 2001 5(2):67–86. [PubMed: 11486655]
20. Kasai M, Kiyama Y, Kawamura A. Application of peripheral blood stem cells (PBSC) mobilized by recombinant human granulocyte colony stimulating factor for allogeneic PBSC transplantation and the comparison of allogeneic PBSC transplantation and bone marrow transplantation. Transfus Apher Sci. Apr; 2002 26(2):121–7. [PubMed: 12121068]
21. Russell NH, Byrne JL. Allogeneic transplantation using peripheral blood stem cells. Best Pract Res Clin Haematol. Dec; 2001 14(4):685–700. [PubMed: 11924916]
22. Spierings E, Vermeulen CJ, Vogt MH, Doerner LE, Falkenburg JH, Mutis T, et al. Identification of HLA class II-restricted H-Y-specific T-helper epitope evoking CD4+ T-helper cells in H-Y-mismatched transplantation. Lancet. Aug 23; 2003 362(9384):610–5. [PubMed: 12944060]
23. Andrade MC, Penedo MC, Ward T, Silva VF, Bertolini LR, Roberts JA, et al. Determination of genetic status in a closed colony of rhesus monkeys (Macaca mulatta). Primates. Jul; 2004 45(3): 183–6. [PubMed: 15103562]
24. O'Leary CE, Wiseman RW, Karl JA, Bimber BN, Lank SM, Tuscher JJ, et al. Identification of novel MHC class I sequences in pig-tailed macaques by amplicon pyrosequencing and full-length cDNA cloning and sequencing. Immunogenetics. Oct; 2009 61(10):689–701. [PubMed: 19777225]
25. Wiseman RW, Karl JA, Bimber BN, O'Leary CE, Lank SM, Tuscher JJ, et al. Major histocompatibility complex genotyping with massively parallel pyrosequencing. Nat Med. Nov; 2009 15(11):1322–6. [PubMed: 19820716]

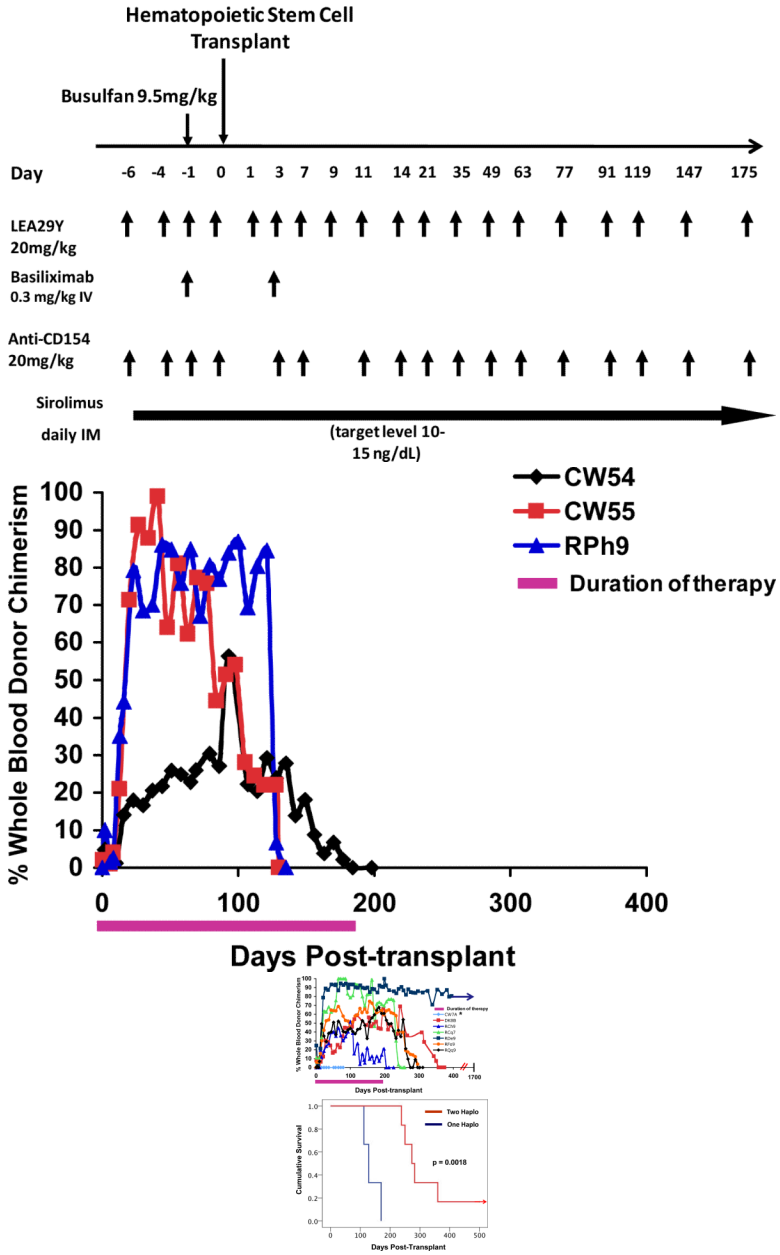

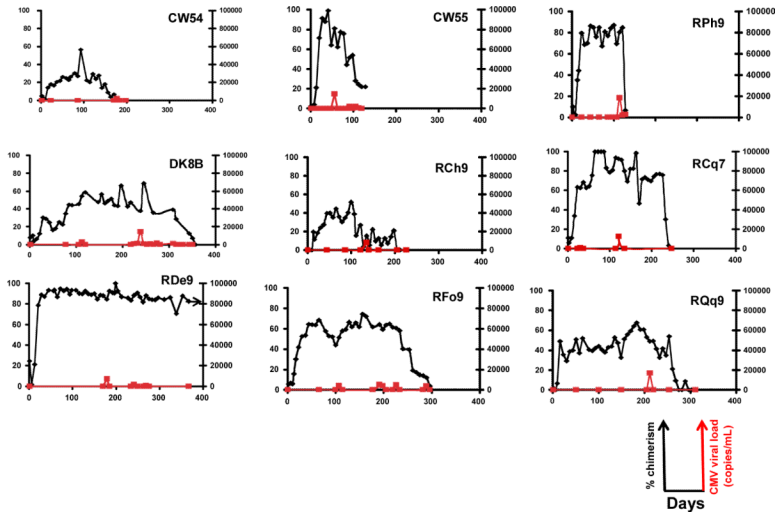

Figure 1. Mixed chimerism-induction after nonmyeloablative HSCT in one- and two-MHC haplotype matched transplant pairs

Figure 1a: Pre-transplant preparation and immunosuppression strategy. Busulfan was given on day -1 at a dose of 9.5mg/kg. The hematopoietic stem cell transplant was given on day 0. The immunosuppressive regimen was given as shown by the arrows in the figure, with each arrow representing an individual dose of drug, at the following concentrations: LEA29Y (20mg/kg), Basiliximab (0.3mg/kg), Anti-CD154 (20mg/kg), sirolimus (once daily dosing was begun at 0.025mg/kg and adjusted to achieve a serum trough level of 10–15mg/mL).

Figure 1b: Longitudinal analysis of whole blood chimerism for one MHC haplotype-matched transplant recipients. DNA was isolated from whole blood, which was collected on the days indicated in the figure. The percentage of donor chimerism was determined by quantitative PCR for sex-determined or MHC-specific alleles that were disparate between the donor and recipient.

Figure 1c: Longitudinal analysis of whole blood chimerism for two MHC-haplotype-matched transplant recipients. DNA was isolated from whole blood, which was collected on the days indicated in the figure. The percentage of donor chimerism was determined by determining the ratio of peak heights for donor-or recipient-specific microsatellite amplicons. * CW7A was a control transplant: this animal was given the same pre-transplant preparation with busulfan, along with donor hematopoietic stem cells, but was given no post-transplant immunosuppression.

Figure 1d: Kaplan-Meier analysis reveals prolonged graft survival in the two MHC-haplotype matched cohort compared to the one MHC-haplotype matched cohort. The day of graft loss was defined as the last day that donor chimerism could be detected in DNA purified from the recipient's whole blood. Red lines depict the survival curve for the two-haplotype matched cohort. Blue lines depict the survival curve for the one-haplotype matched cohort. The graft survival measured in these two groups were statistically different, $p = 0.0018$

Figure 1e: Efficient control of CMV in the transplanted animals. A comparison of chimerism and CMV viral load is shown for all transplanted animals. CMV viral load was determined by quantitative PCR and expressed as copies per milliliter of whole blood. Chimerism was determined either by quantitative PCR for donor-specific sex-determined or MHC alleles (for CW54, CW55 and RPh9) or by the ratio of microsatellite peak heights between donor and recipient-specific amplicons (for DK8B, RCh9, RCq7, RDe9, RFo9, and RQq9) and expressed as the percent donor chimerism in the whole blood. Black lines: Donor whole blood chimerism. Red lines: CMV viral load.

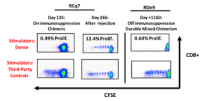

Figure 2. Alloproliferation was inhibited in the presence of mixed chimerism and tolerance, but re-emerged in the setting of transplant rejection

Shown are representative CFSE MLR assays (analyzed after five days of cell culture) for animal RCq7 andRDe9. X axis: CFSE fluorescence. Y axis: CD8+ Fluorescence. Top row: CFSE MLR using donor cells as stimulators. Bottom row: CFSE MLR using third party cells as stimulators. Left and middle columns: RCq7. Right column: RDe9. For RCq7, alloproliferation against donor was inhibited while the animal remained on immunosuppression and displayed mixed-chimerism, while alloproliferation against third party stimulators was preserved. In the setting of rejection (middle panel), alloproliferation against donor cells re-emerged. For RDe9, inhibition of alloproliferation against donor cells remained for as many as 1160 days post-transplant, while alloproliferation against third party antigens was preserved.

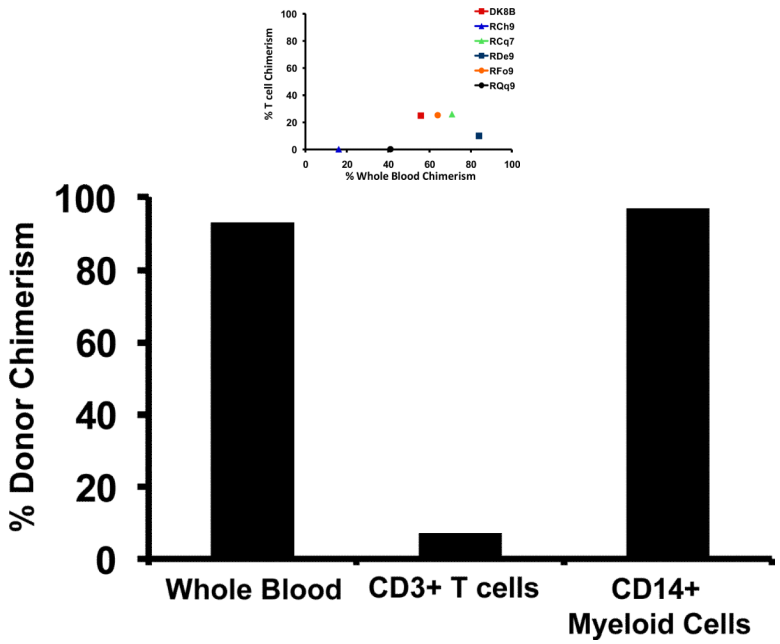

Figure 3. Reduced T cell chimerism compared to whole blood chimerism in two-MHC haplotype matched transplants

Figure 3a: Comparison of whole blood chimerism and T cell chimerism. For whole blood, the percentage of donor chimerism was determined by quantifying the ratio of peak heights for donor-or recipient-specific microsatellite amplicons after purification of DNA from the unfractionated whole blood. For T cell chimerism, CD3+/CD20- cells were first sorted using a FACSAria flow cytometric cell sorter, and then DNA was prepared from these sorted cells. The percentage donor chimerism was then determined by determining the ratio of peak heights for donor-or recipient-specific microsatellite amplicons. Y-axis: Peak T cell chimerism measured while on immunosuppression. X-axis: Whole blood chimerism measured at the same time-point as the T cell chimerism. Each animal is depicted once, as a color-coded point.

Figure 3b: CD14+ myeloid chimerism closely resembles whole blood chimerism. Shown is a representative result from RDe9 (day 56 post-transplant), in which donor chimerism was measured in whole blood, and in flow-cytometrically sorted CD3+ T cells and CD14+ myeloid cells.

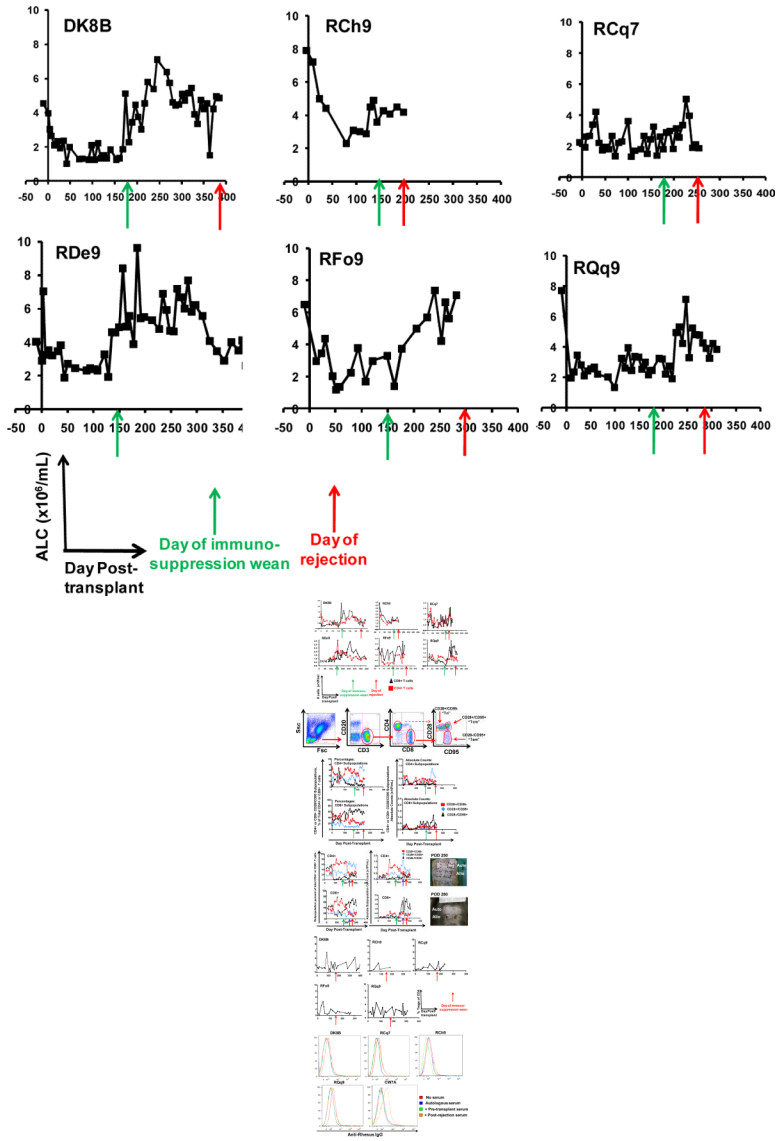

Figure 4. Immunophenotypic analysis reveals a surge of CD4+ Tcm and CD8+Tem that accompanies immunosuppression withdrawal

Figure 4a: Longitudinal analysis of the absolute lymphocyte count (ALC) in the two-haplotype matched pairs. ALC was determined from automated CBC analysis and manual differential counts. x-axis: Days post-transplant. y-axis: ALC. Green arrow: day of the start of immunosuppression weaning. Red arrow: day of rejection.

Figure 4b: Longitudinal analysis of the absolute CD4+ and absolute CD8+ counts in the two-haplotype matched pairs. The absolute CD4+ and CD8+ counts were determined by multiplying the ALC by the fraction of CD3+/CD4+ or CD3+/CD8+ cells, which were determined by flow cytometric analysis. Red squares: CD4+ T cells. Black Triangles: CD8+ T cells. X-axis: Day post-transplant. Y-axis: absolute cell counts. Green arrow: day of the start of immunosuppression weaning. Red arrow: day of rejection. n/a = not analyzed.

Figure 4c: Representative flow cytometric analysis of CD4+ and CD8+ T cell subpopulations. Whole blood was labeled with directly fluorescently-conjugated monoclonal antibodies and then analyzed in the flow cytometer. Lymphocytes were first identified by their forward scatter (Fsc) and Side scatter (Ssc) characteristics. Lymphocytes were then

analyzed for their expression of CD3/CD20/CD4/CD8/CD95 and CD28. CD8+/CD3+ or CD4+/CD3+ cells are identified as shown in the panel above (third from the left). After gating for either CD4+/CD3+ cells (not shown) or CD8+/CD3+ (right panel), the expression of CD28 and CD95 was queried. Antigen inexperienced cells ("Tn") were identified by their expression of CD28 and their lack of expression of CD95. Antigen experienced cells upregulated CD95 and could be distinguished as either CD28 + ("Tcm") or CD28− ("Tem").

Figure 4d: Representative Longitudinal analysis of the relative percentages and the absolute numbers of CD4+ and CD8+ Tn (CD28+/CD95−, red squares), Tcm (CD28+/CD95+, blue diamonds) and Tem (CD28-/CD95+, black triangles) subpopulations. Shown is the analysis for RCq7. The absolute counts of the subpopulations were determined by multiplying the absolute CD4+ or CD8+ counts by the fractions of each subpopulation, determined by flow cytometric analysis. Top row: CD4+ Subpopulations. Bottom Row: CD8+ Subpopulations. Left column: percent of each subpopulation over time. Right column: absolute cell counts for each population over time. Green arrow: day of the start of immunosuppression weaning. Red arrow: day of rejection.

Figure 4e: Longitudinal analysis of the relative percentages and the absolute numbers of CD4+ and CD8+ Tn (CD28+/CD95−, red squares), Tcm (CD28+/CD95+, blue diamonds) and Tem (CD28−/CD95+, black triangles) subpopulations in RQq9, who received a skin allograft after weaning of immunosuppression. The absolute counts of the CD4+ or CD8+ subpopulations were determined by multiplying the absolute CD4+ or CD8+ counts by the fractions of each subpopulation, determined by flow cytometric analysis. Top row: CD4+. Bottom Row: CD8+. Green arrow: day of the start of immunosuppression weaning. Purple arrow: Day 250: day of skin graft. Red arrow: Day of bone marrow rejection.

Figure 4f: Longitudinal analysis of the percentage of CD4+/CD3+/FoxP3+/CD25+ Tregs compared to total CD4+ cells. Whole blood was labeled with antibodies to CD4, CD3, FoxP3 and CD25. CD3+/CD4+ cells were identified, and then the percentage of these cells that were FoxP3+/CD25+ was determined using FloJo flow cytometry analysis software. x-axis: Days post-transplant. y-axis: % Tregs of total CD4+ T cells. Red arrow: day of the start of immunosuppression weaning.

Figure 4g: Anti-donor antibody was not detected in transplant recipients treated with sirolimus and costimulation blockade. The presence of anti-donor antibody was determined by incubating PBMCs from the donor with serum from the recipient which was collected either pre-transplant or after rejection. Anti-donor antibody was then detected flow cytometrically on CD3+/CD20− cells by binding of a FITC-labeled goat anti-monkey IgG to the donor cells to which anti-donor antibodies were bound. Shown are histograms of FITC-fluorescence resulting from the binding of a FITC-labeled Anti-Rhesus IgG to donor cells which were first incubated alone (red traces), pretreated with autologous donor serum (blue traces), pretreated with recipient serum collected pre-transplant (green traces) or with recipient serum collected after rejection (orange traces).

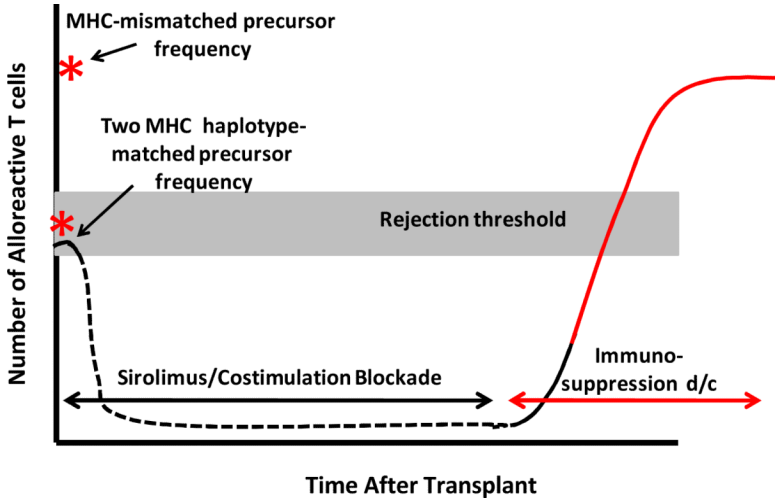

Figure 5. Model of rejection risk in two MHC-haplotype-matched transplants, in the setting of compartmentalized mixed-chimerism and immunosuppression withdrawal

Black solid line: precursor frequency prior to transplant. Black dashed line: decreased number and function of alloreactive T cells during costimulation blockade and sirolimus treatment. Red solid line: acquisition of alloreactivity during post-immunosuppression withdrawal and T cell expansion.

Table 1

Graft composition for two MHC haplotype-matched (top) and one MHC haplotype-matched transplants (bottom).

Recipient	Sex/Age at Transplant	Donor	Sex/Age at Transplant	Stem Cell Source	TNC/kg	CD34/kg	CD3/kg	CD8/kg	CD4/kg
CW7A	F/ 3 yrs	CW7E	F/ 3 yrs	PBSC	1.54×10^{9}	1.42×10^{8}	1.25×10^{8}	8.21×10^{7}	2.73×10^{7}
DK8B	M/ 3 yrs	CW5R	M/ 4 yrs	PBSC	3.61×10^{8}	1.85×10^{7}	1.00×10^{7}	3.76×10^{6}	4.70×10^{6}
RCh9	M/ 4 yrs	RJT7	F/ 6 yrs	PBSC	2.51×10^{9}	8.91×10^{7}	2.66×10^{8}	1.19×10^{8}	1.47×10^{8}
RCq7	F/ 7 yrs	RAI9	M/ 5 yrs	PBSC	7.70×10^{8}	4.44×10^{7}	8.32×10^{7}	3.64×10^{7}	3.50×10^{7}
RDe9	F/ 3 yrs	RNs9	F/ 2 yrs	BM	1.43×10^{9}	6.60×10^{7}	8.57×10^{7}	4.79×10^{7}	4.63×10^{7}
RFo9	M/ 3 yrs	RII8	F/ 5 yrs	PBSC	1.94×10^{8}	2.27×10^{7}	4.24×10^{7}	2.29×10^{7}	1.96×10^{7}
RQq9	M/ 4 yrs	RKg7	F/ 8 yrs	PBSC	7.01×10^{8}	1.84×10^{7}	2.39×10^{7}	1.16×10^{7}	1.22×10^{7}
DJ66	M/ 4 yrs	CT99	M/ 6 yrs	BM	2.19×10^{9}	1.30×10^{8}	1.60×10^{8}	7.90×10^{7}	1.50×10^{7}
DJ63	M/ 3 yrs	CX15	F/ 4 yrs	BM	2.53×10^{9}	1.30×10^{8}	1.10×10^{8}	4.10×10^{7}	3.50×10^{7}
One-MHC Haplotype Matched									
CW54	M/ 3 yrs	CW5X	M/ 3 yrs	BM	1.72×10^{9}	1.58×10^{8}	6.96×10^{7}	5.29×10^{7}	1.03×10^{7}
CW55	M/ 2 yrs	CW5P	F/ 2 yrs	BM	2.10×10^{9}	1.23×10^{8}	1.52×10^{8}	9.02×10^{7}	6.14×10^{7}
RPh9	F/ 4 yrs	RMC4	M/ 13 yrs	PBSC	8.33×10^{8}	1.03×10^{8}	8.03×10^{7}	4.77×10^{7}	3.26×10^{7}

Am J Transplant. Author manuscript; available in PMC 2011 November 1.